Neuron, Volume *73*

Supplemental Information

GlialCAM, a Protein Defective in a Leukodystrophy, Serves as ClC-2 Cl^- Channel Auxiliary Subunit

Elena Jeworutzki, Tania López-Hernández, Xavier Capdevila-Nortes, Sònia Sirisi, Luiza Bengtsson, Marisol Montolio, Giovanni Zifarelli, Tanit Arnedo, Catrin S. Müller, Uwe Schulte, Virginia Nunes, Albert Martínez, Thomas J. Jentsch, Xavier Gasull, Michael Pusch, Raúl Estévez

Inventory of Supplemental Items

Figure S1
Related to Figure 1; contains proteomic information.

Figure S2
Related to Figure 2; contains localization of the studied proteins in a knock-out mouse model.

Figure S3
Related to Figure 3; shows the surface expression levels of the proteins depicted in Figure 3.

Figure S4
Related to Figure 4; shows that GlialCAM alone does not induce any currents above background in *Xenopus* oocytes and HEK cells and that the increase of currents after GlialCAM overexpression in astrocytes is not due to effects on gap junction proteins.

Figure S5
Related to Figure 6; shows the behaviour of deletion mutants of ClC-2 and GlialCAM.

Figure S6
Related to Figure 7; contains additional information on the interaction and the function of several GlialCAM variants containing MLC-related mutations.

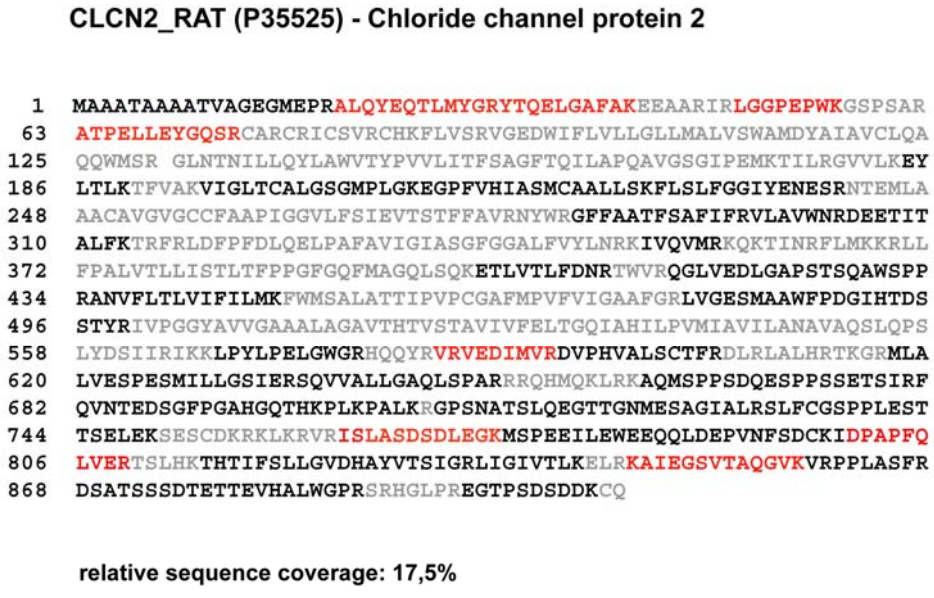

Figure S1. Proteomic identification of ClC-2 as a binding partner of GlialCAM.
Coverage of the primary sequence of ClC-2 by mass spectrometry. Amino acid sequence was taken from the SwissProt database (accession number given in brackets); peptides accessible to and identified by nano-LC-MS/MS (as described in Methods) are in red; those accessible but not identified are in black; peptides not accessible to the LC-MS/MS setup used are given in grey and were not considered for the calculation of relative sequence coverage. Related to Figure 1.

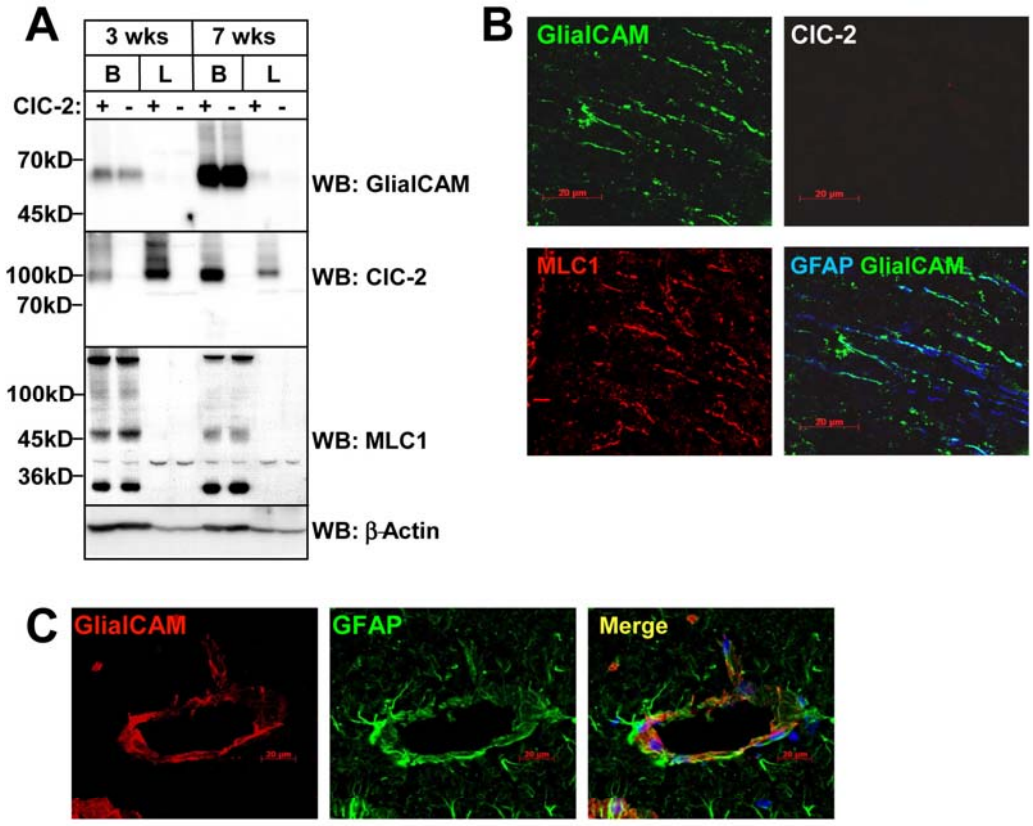

Figure S2. Expression and localization of MLC1 and GlialCAM in ClC-2 KO mice.
A, Brains (B) and livers (L) of 3 and 7 weeks old ClC-2 wild-type and KO mice were lysed and proteins separated by SDS PAGE. ClC-2, GlialCAM and MLC1 were detected on blots with specific antibodies. Immunodetection of β-Actin served as a control for equal loading. The panel shown is representative for three independent experiments.
B, C, Brain sections from 4 weeks old ClC-2 KO mice were stained with GFAP, ClC-2, MLC1 and GlialCAM antibodies as indicated. **b,** Bergmann glia in the molecular layer of the cerebellum; **c,** blood vessels in the hippocampus. Lack of ClC-2 staining in Clcn2-/- tissue confirms the specificity of the antibodies.
Related to Figure 2.

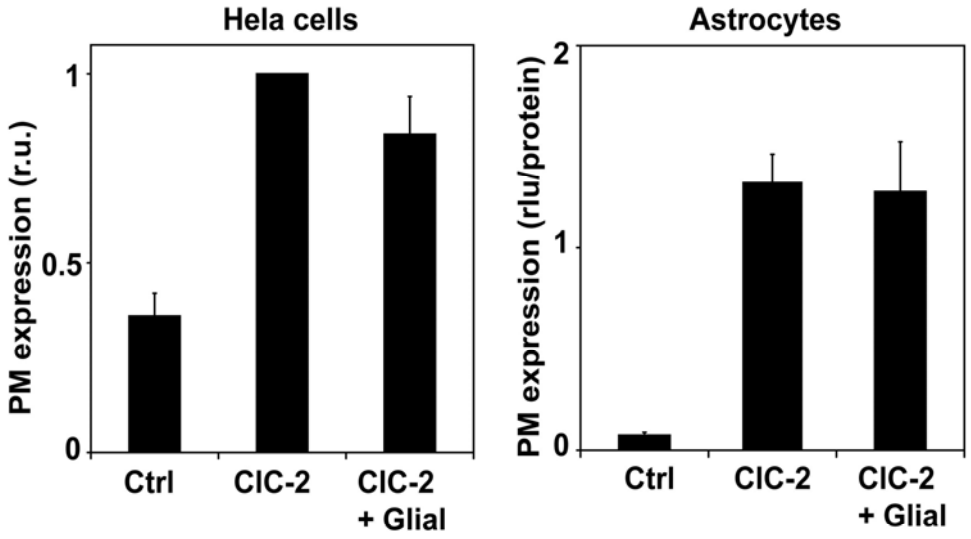

Figure S3. GlialCAM does not modify surface levels of ClC-2 in HeLa cells or primary astrocytes. Surface expression of epitope-tagged ClC-2 in the presence and absence of GlialCAM in HeLa cells or astrocytes. HeLa Cells were transfected with ClC-2 containing an added extracytosolic HA tag. Primary astrocytes were transduced with an adenovirus expressing the same protein. Surface expression was ascertained in a chemiluminescence assay. From four independent experiments in HeLa cells and two experiments in primary astrocytes, no statistical differences were observed between ClC-2 with or without GlialCAM. Here we show average data from HeLa cells, normalized with the expression of ClC-2 alone, and a typical experiment from primary astrocytes.
Related to Figure 3.

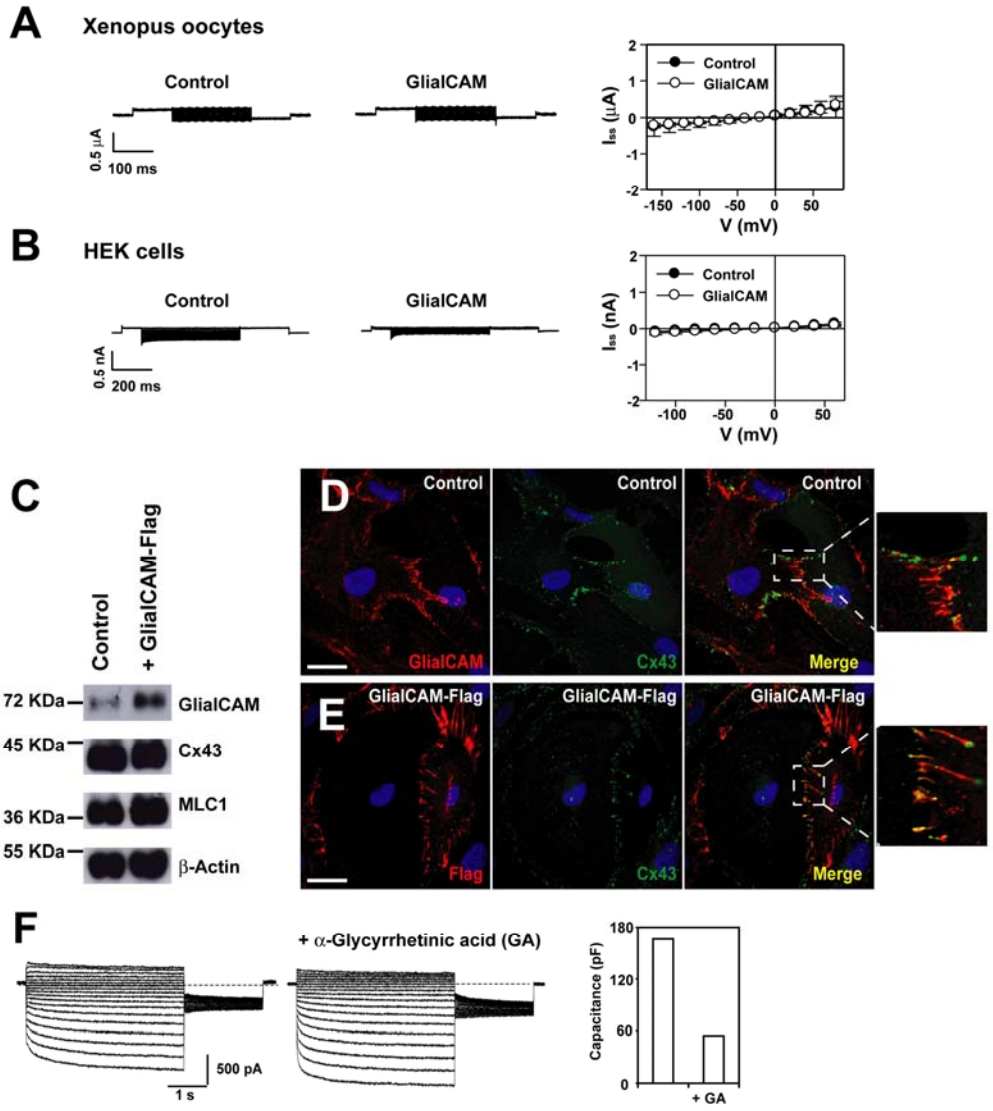

Figure S4. Expression of GlialCAM alone does not activate gap junctions.

A, Typical voltage-clamp traces of control oocytes and GlialCAM-injected oocytes. Right panel, average steady-state current-voltage relationship of control (filled circles) and GlialCAM injected oocytes (open circles). Data are from 2 batches of oocytes with n=4 from each batch; error bars indicate SEM. In the same batches, the activity of the GlialCAM RNA was positively tested by co-injection with ClC-2 in separate oocytes.

B, Typical voltage-clamp traces of control (untransfected) and GlialCAM-transfected HEK cells. Right panel, average steady-state current-voltage relationship of control (filled circles) and GlialCAM::emGFP transfected HEK cells (open circles). Data are from 2 independent transfections (n=4/5 cells each); error bars indicate SEM. Transfection efficiency was positively tested by parallel transfections of ClC-2 with GlialCAM.

C, Over-expression of GlialCAM in primary astrocytes does not modify expression levels of Connexin 43 (Cx43), as assesed by Western blot analysis. Two other independent experiments gave similar results.

D, Immunolocalization in primary astrocytes (control) of endogenous GlialCAM and Cx43. The inset shows a magnification of astrocyte processes, which indicates that both proteins do not overlap significantly. Nuclei were stained with DAPI (blue). Scale bar: 20 µm.

E, Over-expression of flag-tagged GlialCAM in primary astrocytes does not modify the subcellular localization of Cx43. Scale bar: 20 µm. The inset shows a magnification of astrocyte processes, showing that there is no change in the localization of Cx43.

F, Representative traces of chloride currents of dbcAMP-treated astrocytes transduced with adenoviruses expressing GlialCAM fused to GFP which were coupled to neighboring astrocytes before and after application of 25 µM 18α-Glycyrrhetinic acid (GA). The right panel shows the capacitance before and after GA application for this cell. From four independent measurements capacitance values were reduced from 148 ± 21 pF to 85 ± 31 pF after GA application. In contrast, at -120 mV, the ionic current value was 1456 ± 153 pA and 1427 ± 204 pA, before and after GA application.

Related to Figure 4.

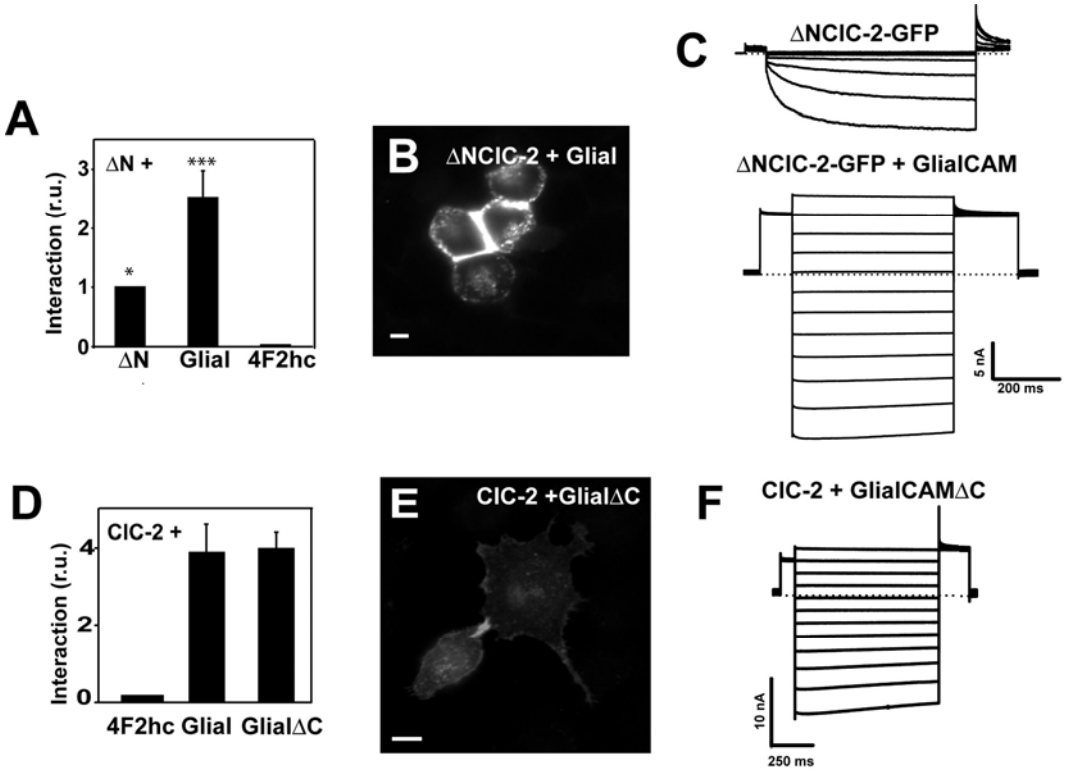

Figure S5. Insights into the mechanism of ClC-2 activation by GlialCAM.
A, Interaction between ΔNClC-2 and ΔNClC-2 or GlialCAM was monitored using split-TEV interaction assays. 4F2hc was used as a negative control. The result is an average of 7 independent experiments. * $p < 0.05$; *** $p < 0.001$ vs 4F2hc.
B, GlialCAM changed the subcellular distribution of ΔNClC-2 in transiently transfected HeLa cells. Scale bar: 20 μm.
C, Typical whole-cell voltage clamp current traces of cells transfected with ΔNClC-2-GFP together with GlialCAM. The GFP tag does not affect ΔNClC-2 current properties. ΔNClC-2 alone retains hyperpolarization activation in the patch clamp recordings, even though being much faster than wild-type ClC-2 (compare with Figure 4C).
D, Interaction between ClC-2 and GlialCAM or GlialCAM-ΔC was monitored using split-TEV interaction assays. 4F2hc was used as a negative control. The result is an average of 5 independent experiments. No significant differences between GlialCAM and the C-terminal deletion mutant GlialCAM-ΔC were found.
E, GlialCAM-ΔC changed the subcellular distribution of ClC-2 in transiently transfected HeLa cells. Scale bar: 20 μm.
F, Currents mediated by ClC-2 together with GlialCAM-ΔC expressed in transfected HEK-293 cells. Related to Figure 6.

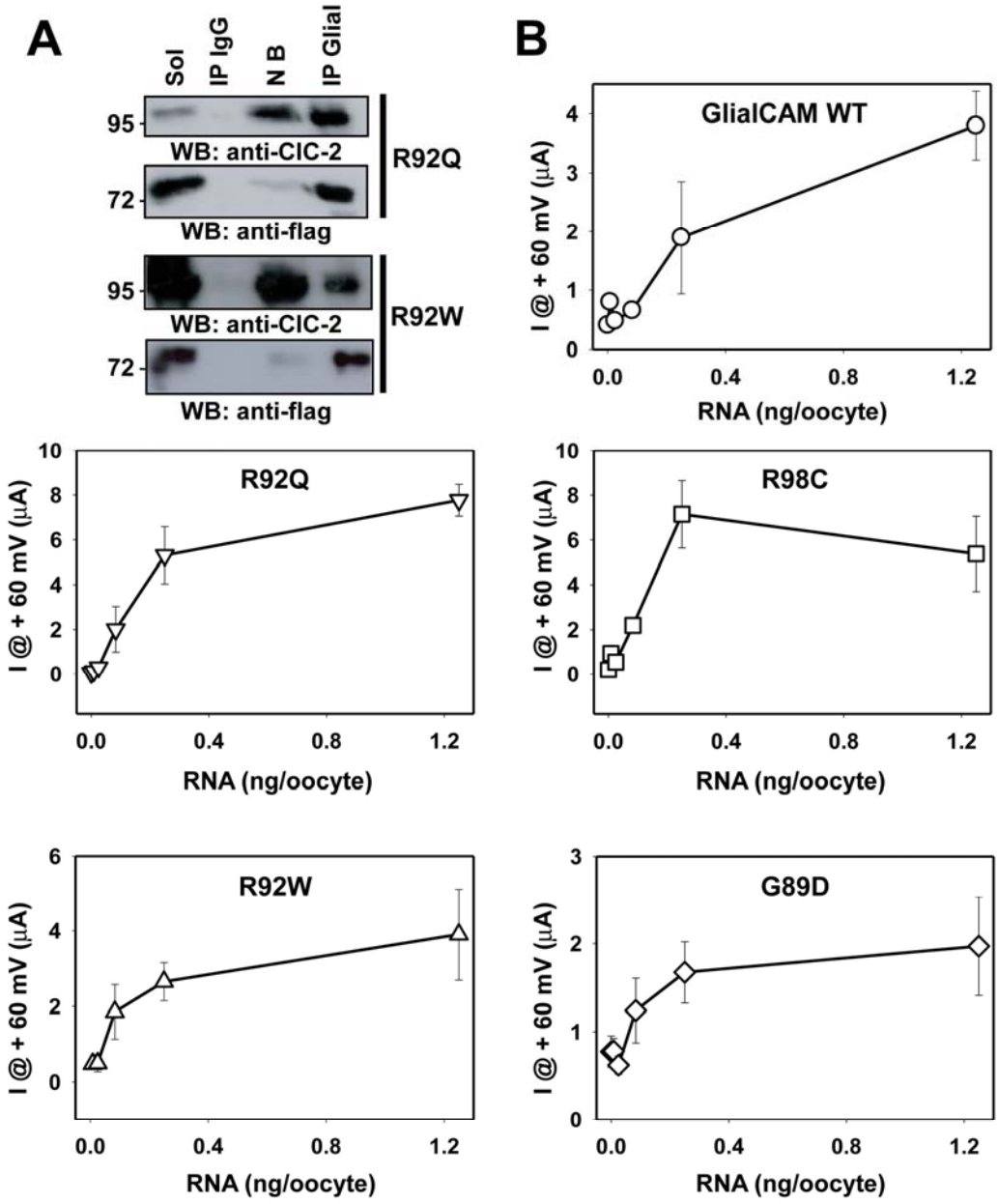

Figure S6. GlialCAM containing MLC-related mutations interact biochemically and functionally with ClC-2.

A, Immunoprecipitation was performed using extracts from HeLa cells transfected with ClC-2 and the indicated GlialCAM variants C-terminally flag tagged. Similar results were seen in two experiments.

B, Increasing amounts of WT and GlialCAM containing MLC-related mutations RNA were co-injected with 5 ng ClC-2 RNA and the average instantaneous current at +60 mV is plotted as a function of the amount of GlialCAM RNA injected. The panels show typical experiments from one batch of oocytes each. Similar results were obtained in at least three batches of oocytes for each construct. Every measuring point represents n = 5 ± SEM. All variants are qualitatively equally effective as WT GlialCAM in activating ClC-2.

Related to Figure 7.